Food and Chemical Toxicology 123 (2019) 349–362

Contents lists available at ScienceDirect

Food and Chemical Toxicology

journal homepage: www.elsevier.com/locate/foodchemtox

Tetrahydrocurcumin and octahydrocurcumin, the primary and final hydrogenated metabolites of curcumin, possess superior hepatic-protective effect against acetaminophen-induced liver injury: Role of CYP2E1 and Keap1-Nrf2 pathway

Dan-Dan Luo[a,1], Jin-Fen Chen[a,1], Jing-Jing Liu[a], Jian-Hui Xie[b], Zhen-Biao Zhang[c], Jiang-Yong Gu[d], Jian-Yi Zhuo[a], Song Huang[a], Zi-Ren Su[a,e,*,2], Zhang-Hua Sun[a,**,2]

[a] Guangdong Provincial Key Laboratory of New Drug Development and Research of Chinese Medicine, Mathematical Engineering Academy of Chinese Medicine, Guangzhou University of Chinese Medicine, Guangzhou, 510006, PR China
[b] Guangdong Provincial Key Laboratory of Clinical Research on Traditional Chinese Medicine Syndrome, The Second Affiliated Hospital, Guangzhou University of Chinese Medicine, Guangzhou, 510120, PR China
[c] School of Chinese Medicine, Faculty of Medicine, The Chinese University of Hong Kong, Shatin, N.T, Hong Kong SAR, PR China
[d] The Second Clinical College of Guangzhou University of Chinese Medicine, Guangzhou, 510120, PR China
[e] Dongguan Mathematical Engineering Academy of Chinese Medicine, Guangzhou University of Medicine, Dongguan, 523808, PR China

ARTICLE INFO

Keywords:
Octahydrocurcumin
Tetrahydrocurcumin
Acetaminophen
Oxidative stress
Keap1-Nrf2
CYP2E1

ABSTRACT

Acetaminophen (APAP) overdose-induced hepatotoxicity is tightly associated with oxidative stress. Tetrahydrocurcumin (THC) and octahydrocurcumin (OHC), the primary and final hydrogenated metabolites of curcumin (CUR), possess stronger antioxidant activity *in vitro*. The present study was performed to investigate the potential and mechanism of OHC and THC against APAP-induced hepatotoxicity in parallel to CUR. Our results showed that OHC and THC dose-dependently enhanced liver function (ALT and AST levels) and alleviated histopathological deterioration. Besides, OHC and THC significantly restored the hepatic antioxidant status by miring level of MDA and ROS, and elevated levels of GSH, SOD, CAT and T-AOC. In addition, OHC and THC markedly suppressed the activity and expressions of CYP2E1, and bound to the active sites of CYP2E1. Moreover, OHC and THC activated the Keap1-Nrf2 pathway and enormously enhanced the translational activation of Nrf2-targeted gene (GCLC, GCLM, NQO1 and HO-1) against oxidative stress, via inhibiting the expression of Keap1 and blocking the interaction between Keap1 and Nrf2. Particularly, OHC and THC exerted superior hepato-protective and antioxidant activities to CUR. In conclusion, OHC and THC possess favorable hepato-protective effect through restoring antioxidant status, inhibiting CYP2E1 and activating Keap1-Nrf2 pathway, which might represent promising antioxidants for the treatment of APAP-induced hepatotoxicity.

1. Introduction

Tetrahydrocurcumin (THC, Fig. 1B) and octahydrocurcumin (OHC, Fig. 1C), the food-derived antioxidants, are the primary and final hydrogenated metabolites of curcumin (CUR, Fig. 1A). CUR is a popular cooking spice, food pigment, and flavouring agent derived from the rhizome of *Curcuma longa*, which is widely used for the treatment of liver disorders (Ireson et al., 2002; Kocaadam and Sanlier, 2017; Zhao et al., 2015). Nowadays, attention has been focused on OHC and THC due to their similar but superior beneficial properties to CUR, including anti-inflammatory (Zhao et al., 2015), anti-tumor (Liu et al., 2017; Zhang et al., 2018), and especially antioxidant activities (Somparn et al., 2007). THC, the primary and major hydrogenated metabolite of CUR, possesses protective effect against various diseases such as renal damage, diabetes and hypertension (Murugan and Pari, 2010; Nakmareong et al., 2011; Pari and Murugan, 2004; Song et al., 2015).

* Corresponding author. Guangdong Provincial Key Laboratory of New Drug Development and Research of Chinese Medicine, Mathematical Engineering Academy of Chinese Medicine, Guangzhou University of Chinese Medicine, Guangzhou, 510006, PR China.
** Corresponding author.
E-mail addresses: suziren@126.com (Z.-R. Su), sysuszh@126.com (Z.-H. Sun).
[1] These authors contributed equally to this work.
[2] These corresponding authors contributed equally to this work.

https://doi.org/10.1016/j.fct.2018.11.012
Received 7 September 2018; Received in revised form 20 October 2018; Accepted 5 November 2018
Available online 10 November 2018

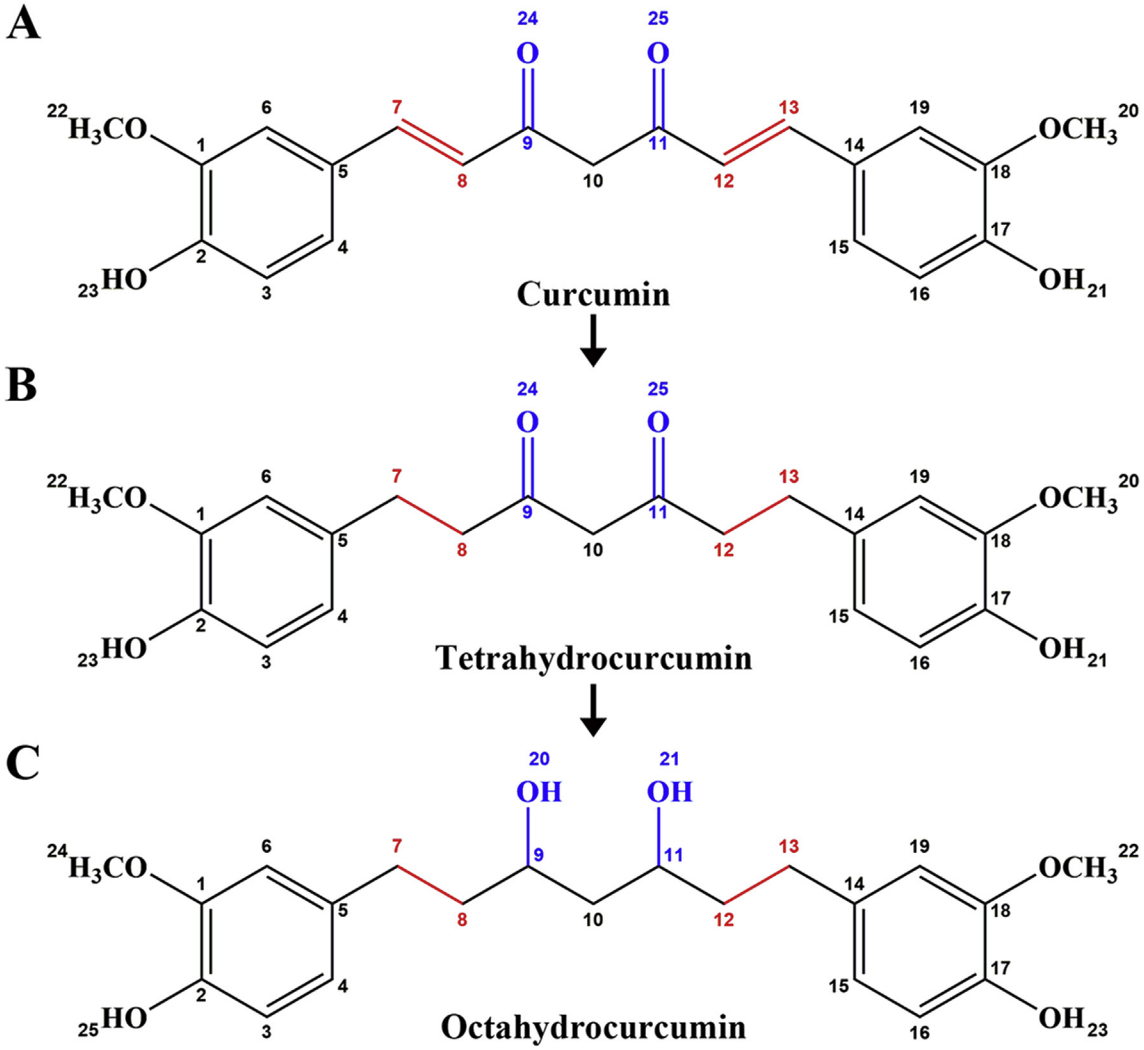

Fig. 1. Chemical structures of (A) Curcumin, (B) Tetrahydrocurcumin and (C) Octahydrocurcumin.

However, the potential hepato-protective effect of THC against acute liver injury remained obscure. OHC, the final hydrogenated metabolite of CUR, is rarely explored largely ascribed to its poor availability.

Acetaminophen (APAP) overdose is a worldwide leading cause of drug-induced hepatotoxicity. APAP toxicity accounts for above 40% of acute liver failure cases in the United States, Great Britain and Europe (Lee, 2017). When taken at therapeutic dose, over 90% of APAP is metabolized into nontoxic products. And about 5–8% of APAP is metabolized into a toxic metabolite, N-acetyl-p-benzoquinoneimine (NAPQI) by the cytochrome P450 system (mainly CYP2E1). Under normal circumstances, NAPQI is rapidly converted to nontoxic products by glutathione (GSH) (Lancaster et al., 2015). However, once APAP is overdosed, excessive NAPQI will be formed, which depletes hepatic GSH stores (Xu et al., 2017). Subsequently, the remaining NAPQI will react with the cellular proteins and cause oxidative stress, microsomal membrane damage, and even cell death (Das et al., 2011).

The Kelch-like ECH-associated protein 1 (Keap1)-nuclear factor erythroid 2 related factor 2 (Nrf2) system plays a critical role in the hepatic oxidative injury, and has been considered as a prospective target for liver diseases. Nrf2 serves as an essential regulator of an array of detoxifying and antioxidant defense genes expression in the liver (Lu et al., 2016). Keap1 is known as a negative regulator of Nrf2 (Kaspar et al., 2009). Under unstressed conditions, Keap1 binds to Nrf2 in the cytoplasm and promotes the degradation of Nrf2. Under oxidative stress, Keap1 is inactivated, while Nrf2 is stabilized. Therefore, the newly synthesized Nrf2 is accumulated and constantly activated (Sha et al., 2015). As a result, Nrf2 translocates into the nucleus and induces the expressions of a battery of cyto-protective genes such as glutamate cysteine ligase catalytic subunit (GCLC), glutamate-cysteine ligase modifier subunit (GCLM), NAD(P)H quinone oxidoreductase 1 (NQO1), and heme oxygenase-1 (HO-1), all of which play an important role in the detoxication of APAP (Sha et al., 2015; Shin et al., 2013).

Oxidative stress is involved in the various toxicities associated with APAP (Wang et al., 2017), and therefore OHC and THC with prominent antioxidant properties may be effective in the suppression of oxidative stress associated with APAP treatment. In the present study, we followed our previous highly effective route to produce OHC (Zhang et al., 2018), and comparatively deciphered the potency and mechanism of OHC and THC against APAP-induced hepatotoxicity. For the first time, OHC was revealed to exert pronounced hepato-protective effect. THC also exhibited appreciable hepato-protective effect against APAP-induced hepatotoxicity. The mechanism was intimately associated with suppressing CYP2E1 through inhibiting its expression and binding to its active sites, maintaining redox homeostasis, and activating the Keap1-Nrf2 antioxidant signaling pathway through inhibiting the expression of Keap1 and blocking the binding of Keap1 to Nrf2, thus triggering the transcriptional and translational activation of Nrf2-mediated antioxidant response elements (Fig. 10). Moreover, OHC and THC possessed superior hepato-protective effect to their progenitor CUR in combating against APAP-induced hepatotoxicity.

Table 1
Primer sequences for target genes.

Gene	Primer sequence (5′–3′)	
	Forward	Reverse
CYP2E1	CGTTGCCTTGCTTGTCTGGA	AAGAAAGGAATTGGGAAAGGTCC
GCLC	TGGCTTTGAGTGCTGCATCT	ATCACTCCCCAGCGACAATC
GCLM	TCACAATGACCCGAAAGAACTG	ACCCAATCCTGGGCTTCAAT
NQO1	GGTTTACAGCATTGGCCACACT	AACAGGCTGCTTGGAGCAAA
HO-1	CAGCCCCACCAAGTTCAAAC	GGCGGTCTTAGCCTCTTCTGT
GAPDH	AGGTCGGTGTGAACGGATTTG	GGGGTCGTTGATGGCAACA

To the best of our knowledge, it was the first study to delineate the hepato-protective effect of OHC and THC in APAP-induced liver injury, and also the innovative endeavor to comparatively explore the anti-oxidant activity of hydrogenated metabolites THC and OHC *in vivo*. Our results might add new dimension to the hepato-protective effect and mechanism of CUR and its metabolites, which further corroborated the medicinal application of turmeric as a functional food in the treatment of hepatic disorders. This insight was envisaged to enlighten the knowledge on the development of food-derived OHC and THC as novel antioxidants for the treatment of APAP-induced liver injury. OHC and THC may serve as promising lead scaffolds for the lead optimization for novel curcumin analogs.

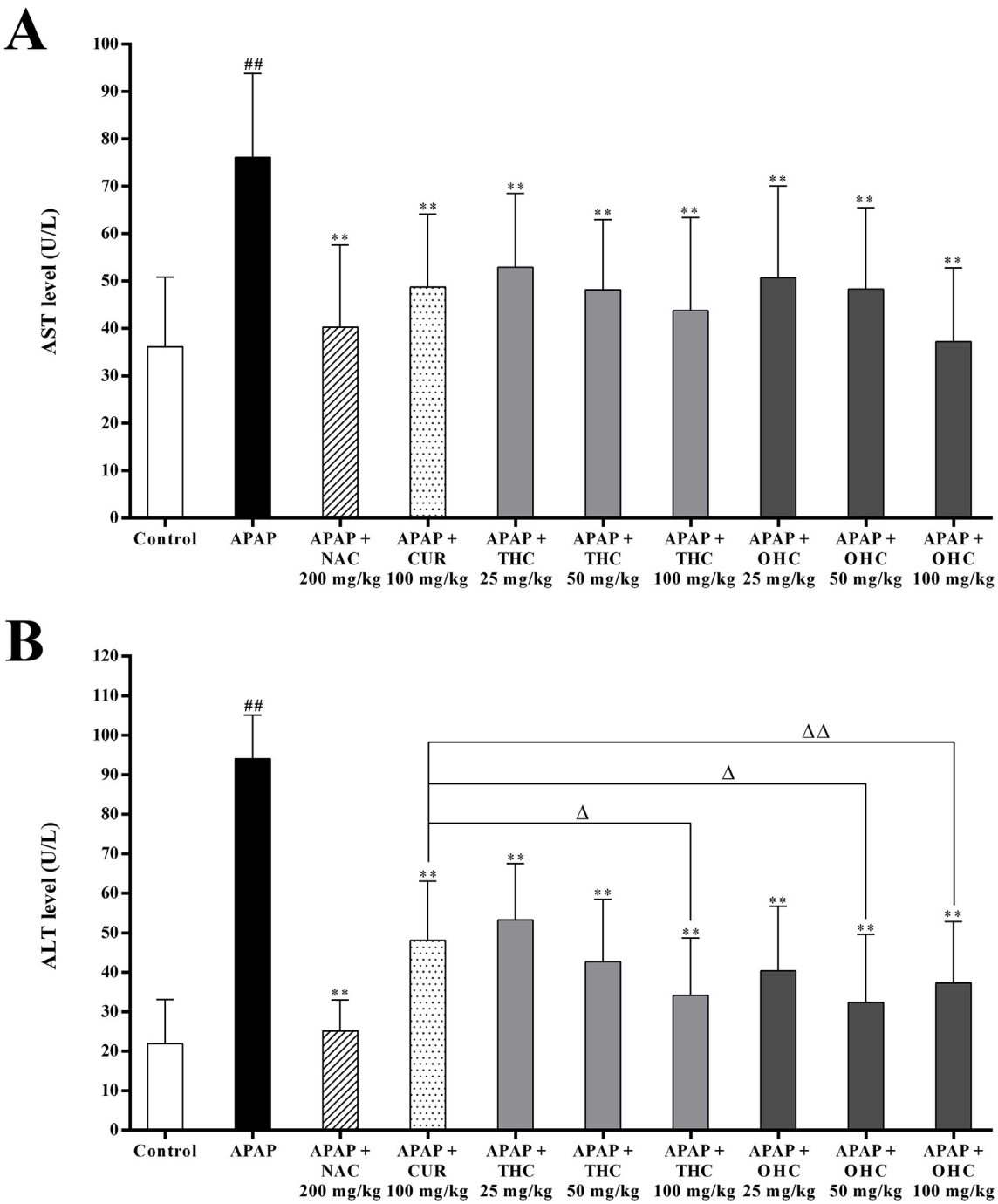

Fig. 2. Differential effects of THC, OHC and CUR on the levels of (A) AST and (B) ALT in serum. Data are presented as the mean ± SD (n = 10). $^{\#\#}p < 0.01$ versus control group. $^{*}p < 0.05$, $^{**}p < 0.01$ versus APAP-treated group. $^{\Delta}p < 0.05$, $^{\Delta\Delta}p < 0.01$ versus treatment of CUR group.

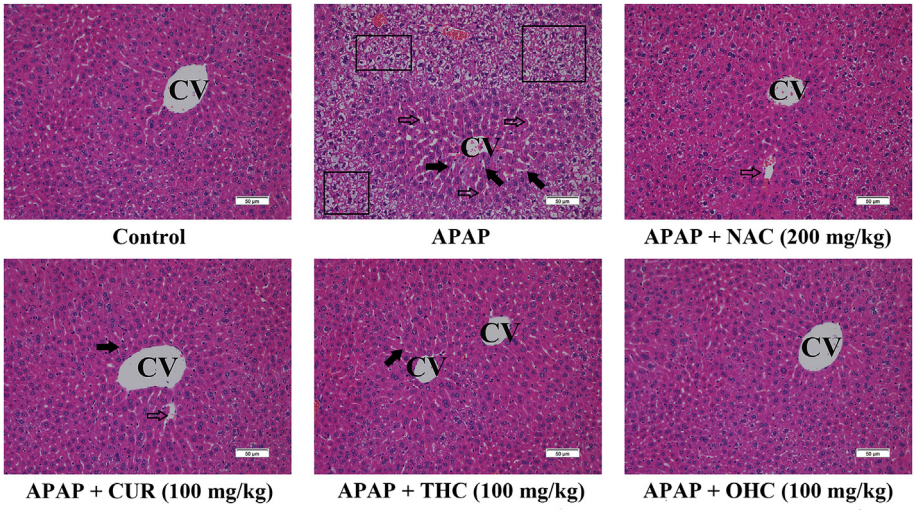

Fig. 3. Differential effects of THC, OHC and CUR on the liver histological alternations (original magnification × 100). CV: central vessel; Solid arrows: inflammatory cell infiltration; Open arrow: sinusoidal dilation; Rectangle: vacuolation. The scale indicates 50 μm.

2. Materials and methods

2.1. Chemical compounds and reagents

Chemical compounds. OHC was synthesized and purified according to our previous report, with purity over 98.0% (Zhang et al., 2018). CUR, THC, APAP, N-acetyl cysteine (NAC), p-nitrophenol, 4-nitrocatechol and NADPH were all purchased from Sigma-Aldrich Chemical Co., Ltd. (St. Louis, MO, USA).

Commercially available kits. Kits for measurement of alanine transaminase (ALT), glutathione (GSH), malondialdehyde (MDA), catalase (CAT), superoxide dismutase (SOD), and total antioxidant capacity (T-AOC) were all purchased from Nanjing Jiancheng Bioengineering Institute (Nanjing, China). Enzyme-linked immunosorbent assay (ELISA) kit for reactive oxygen species (ROS) was obtained from Beijing Andy Huatai Technology Co., Ltd. (Beijing, China).

Reagents for Western blot analysis. Nuclear and cytoplasmic protein extraction kit was purchased from Keygene Biotech Co., Ltd. (Nanjing, China). Radioimmunoprecipitation assay (RIPA) lysis buffer, stripping buffer and bicinchoninic acid (BCA) protein assay kits were obtained from Beyotime Institute of Biotechnology (Shanghai, China). Primary antibodies against CYP2E1, Keap1, Nrf2, GCLC, GCLM, NQO1, heme oxygenase-1 (HO-1), GADPH, Histone H3, and horseradish peroxidase (HRP)-conjugated anti-rabbit secondary antibodies were all obtained from Affinity Biosciences, Cell Signal Transduction (Cambridge, UK). Polyvinylidene difluoride (PVDF) membranes were obtained from GE Healthcare Life Sciences (Pittsburgh, PA, USA).

Reagents for real-time PCR analysis. Trizol reagent was purchased from Thermo Fisher Scientific Inc. (Massachusetts, USA). FastKing RT kit was obtained from Tiangen Biotech Co., Ltd. (Beijing, China). ChamQ Universal SYBR qPCR Master Mix was provided by Vazyme Biotech Co., Ltd. (Nanjing, China). The primer sequences for CYP2E1, GCLC, GCLM, HO-1, NQO1 and GAPDH were from Sangon Biotech Co., Ltd. (Shanghai, China).

2.2. Animals and treatments

Male Kunming mice (20–25 g, 6–8 weeks) were purchased from Guangdong Medical Laboratory Animal Center (Foshan, China). All mice were specific pathogen-free and fed under a standard condition (constant temperature of 24 ± 1 °C and a 12/12 h light-dark cycle) for at least 7 days before the experiment. All animal experiments were performed in accordance with procedures approved by the Animal Experimental Ethics Committee of Guangzhou University of Chinese Medicine (dSPF, 2014021), and the experimental protocols followed the Guide for the Care and Use of Laboratory Animals.

One hundred mice were randomly divided into 10 groups: control (saline, 0.1 ml/10 g, i.g.), APAP (saline, 0.1 ml/10 g, i.g.), NAC (200 mg/kg, i.g.), CUR (100 mg/kg, i.p.), THC (25, 50 and 100 mg/kg, i.p.) and OHC (25, 50 and 100 mg/kg, i.p.). All mice were fasted for 16 h prior to the induction of experimental liver injury. Mice were initially pretreated with corresponding agents. After pretreatment for 30 min, all mice except those in the control group received intraperitoneal injection of APAP (220 mg/kg) to induce liver injury. The dosages used in the present study were selected based on previous studies (Pang et al., 2016; Leong et al., 2012; Liu et al., 2016; Oh et al., 2011) and our pilot trial. After injection of APAP for 12 h, all mice were sacrificed. Blood samples were collected and kept at room temperature for 90 min, and then centrifuged for 15 min (1000 × *g*, 4 °C) to obtain serum. Serum samples were stored at −80 °C for subsequent analysis. Besides, liver tissues were obtained following abdomen dissection. Parts of liver tissues were snap-frozen in liquid nitrogen and stored at −80 °C for subsequent analysis. The same parts of each liver were removed and fixed in 10% buffered formalin for liver histological analysis. To further investigate the underlying mechanism, samples from OHC and THC (100 mg/kg) groups were used for the subsequent studies including histological observation, liver ROS level, CYP2E1 activity, real-time PCR and Western blot analysis.

2.3. Measurement of serum ALT and AST levels

The serum levels of ALT and AST, serving as indicators of liver function, were measured using commercially available kits according to the manufacturer's instructions.

2.4. Measurement of hepatic oxidative stress markers

Liver tissues were thawed and added with saline ice, and then homogenized to obtain 10% liver homogenate. The homogenate was centrifuged for 15 min (2500 rpm, 4 °C) to obtain the supernatant. Subsequently, the supernatant was used for the analyses of MDA, GSH, SOD, CAT, and T-AOC levels by commercially available kits according to the manufacturers' instructions.

2.5. Liver histological observation

The fixed liver tissues were embedded in paraffin, sliced into 5 μm and stained with hematoxylin and eosin following routine procedures.

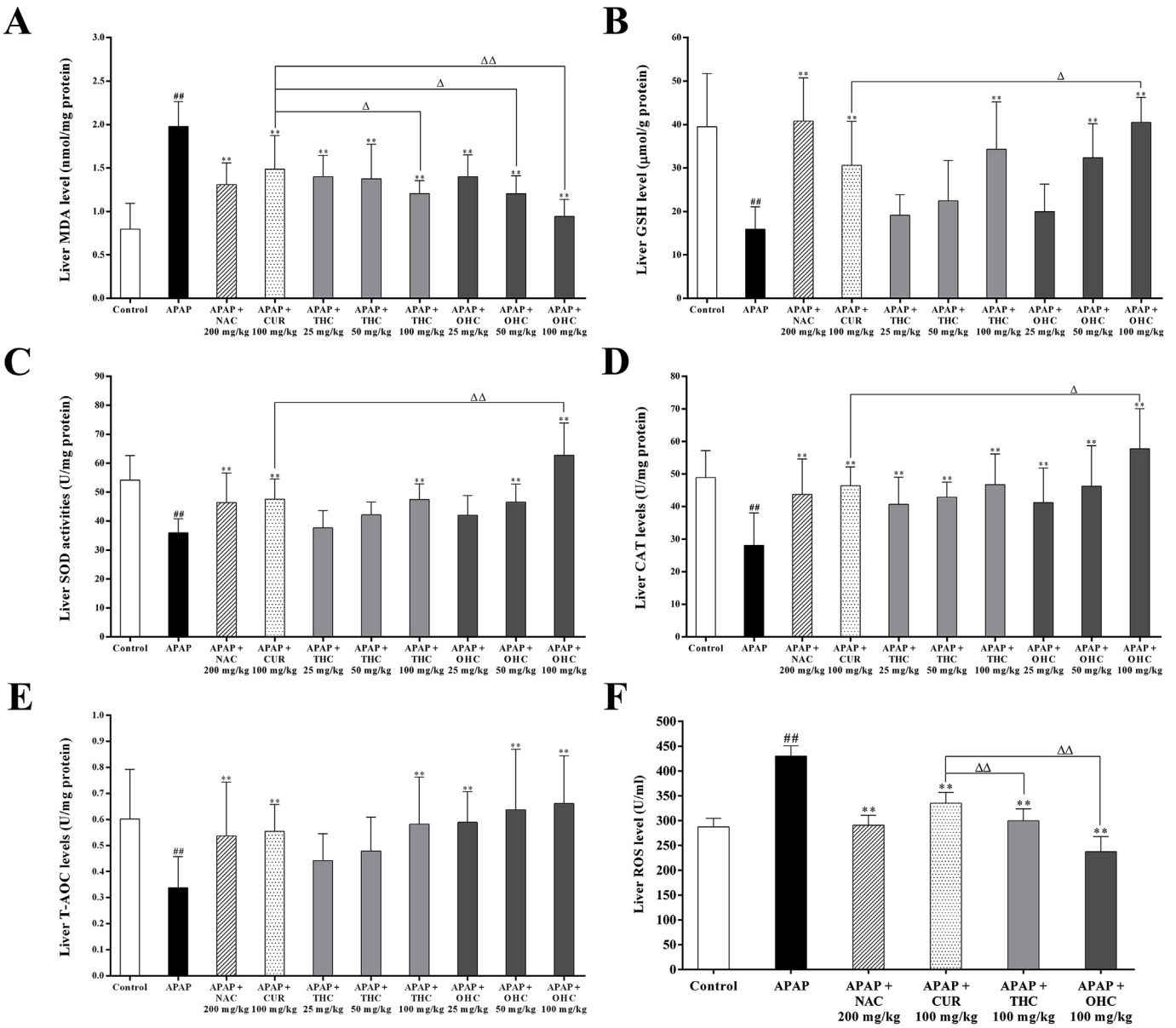

Fig. 4. Differential effects of THC, OHC and CUR on the liver antioxidant status: (A) MDA; (B) GSH; (C) SOD; (D) CAT; (E) T-AOC and (F) ROS. Data are presented as the mean ± SD (n = 10). $^{\#\#}p < 0.01$ versus control group. $^{**}p < 0.01$ versus APAP-treated group. $^{\Delta}p < 0.05$, $^{\Delta\Delta}p < 0.01$ versus treatment of CUR group.

The histological alternations in the hepatic tissues were observed and photographed using an Olympus microscope (BX-46; Olympus, Tokyo, Japan).

2.6. Measurement of liver ROS level

Liver tissues collected from different groups were melted (2–8 °C) and homogenized in ice-cold PBS (pH 7.4). After centrifugation at 3000 rpm for 20 min at 4 °C, the supernatant was collected for ROS measurement using a mouse ROS detection assay kit following the manufacturer's instructions (Kong et al., 2018; Lin et al., 2018).

2.7. Measurement of hepatic CYP2E1 activity

Liver microsomes were isolated following the previous methods with some modifications (Yue et al., 2009). Briefly, liver tissues collected from different groups were melted and homogenized in ice-cold 50 mM Tris with 1.15% (w/v) KCl (pH 7.4). After centrifugation for 20 min (10000 × *g*, 4 °C), the supernatant was collected and centrifuged for 30 min (20000 × *g*, 4 °C). The protein concentration of the final supernatant was determined by the BCA protein assay kit. CYP2E1 activity was determined by measuring the hydroxylation ratio of 4-nitrophenol to 4-nitrocatechol and expressed as pmol/min/mg protein following the previous method (Bray and Rosengren, 2001).

2.8. Protein extraction and western blot analysis

Liver tissues collected from different groups were thawed, homogenized with RIPA lysis buffer, and centrifuged for 5 min (15000 × *g*, 4 °C) to obtain the total protein. The nuclear and cytoplasmic proteins were extracted using a commercially available nuclear and cytoplasmic protein extraction kit in accordance with the manufacturer's instructions. The protein concentration was determined by the BCA protein assay kit and then stored at −80 °C for subsequent Western blot analysis.

Fifty μg of protein was electrophoresed on 6%–12% SDS-PAGE and then transferred onto PVDF membranes. Subsequently, membranes were blocked with 5% skim milk powder in TBST for 1 h, and then

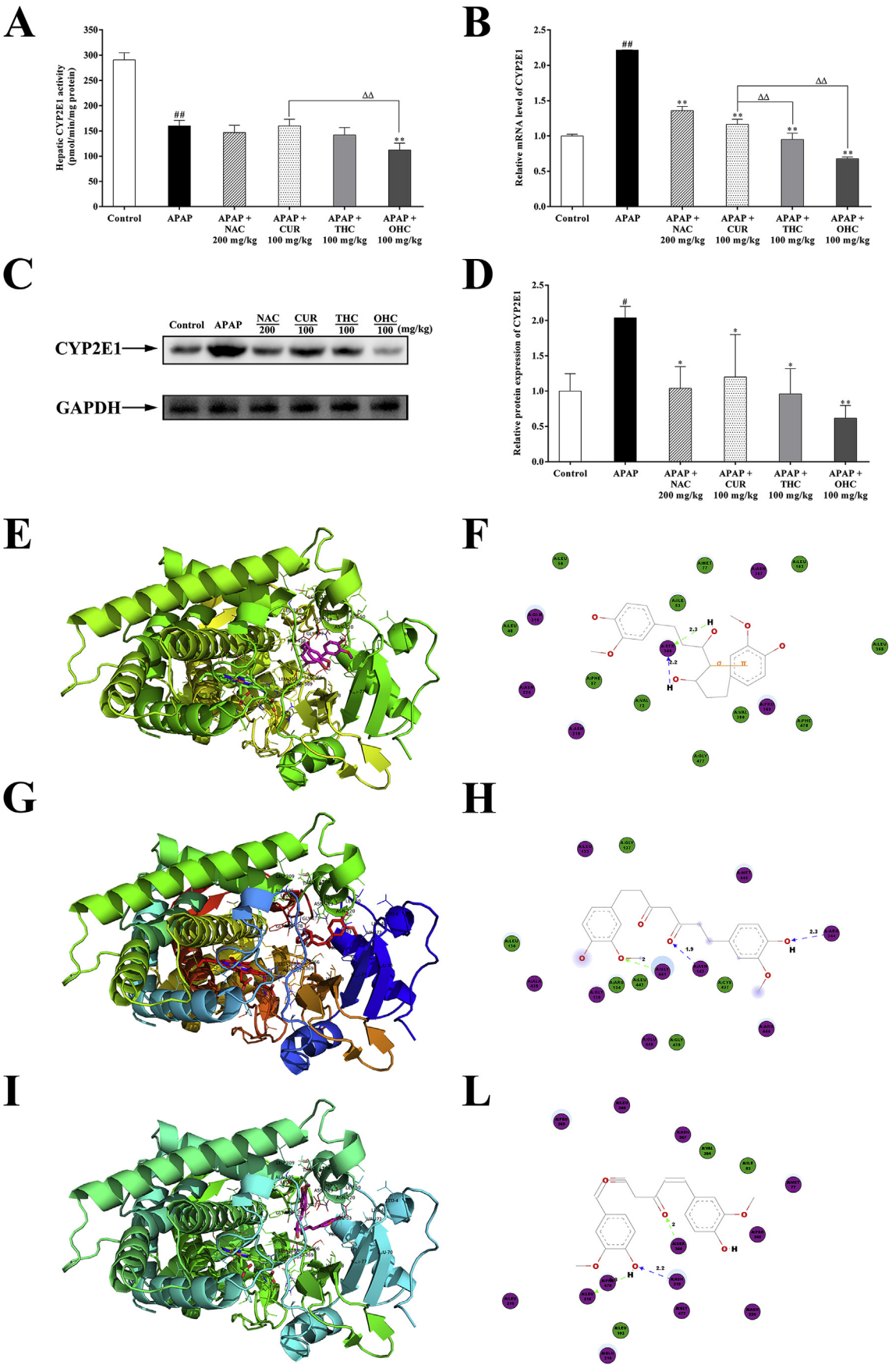

(caption on next page)

Fig. 5. Differential effects of THC, OHC and CUR on CYP2E1 in liver: (A) Enzymatic activities; (B) Densitometry analysis of mRNA level; (C) Representative protein expression band; (D) Densitometry analysis of protein level; (E) 3D and (F) 2D diagrams of the hydrogen bonds interaction between OHC and CYP2E1; (G) 3D and (H) 2D diagrams of the hydrogen bonds interaction between THC and CYP2E1; (I) 3D and (L) 2D diagrams of the hydrogen bonds interaction between CUR and CYP2E1. Data are presented as the mean ± SD (n = 3). $^{\#\#}p < 0.01$ versus control group. $^{*}p < 0.05$, $^{**}p < 0.01$ versus APAP-treated group. $^{\Delta\Delta}p < 0.01$ versus treatment of CUR group.

Table 2
Docking score of OHC, THC and CUR with CYP2E1 and Keap1.

Protein molecules	Chemical compounds	Docking score				
		Lead IT score	H-bond	Amino acid	Ligand atom	H-bond length (Å)
CYP2E1 (PDB ID: 3E6I)	OHC	−6.11	2	SER366	H20	2.2
					H21	2.3
	THC	−5.70	3	ARG344	H21	2.3
				GLY441	O22	2.0
				ASN143	O25	1.9
	CUR	−6.21	3	LEU215	H21	4.8
				ASN219	O21	2.2
				SER366	O24	2.0
Keap1 (PDB ID: 5FNU)	OHC	−5.11	4	LEU365	H22	1.8
				VAL606	O22	2.0
				GLY367	O22	2.3
					H23	2.3
	THC	−7.01	4	VAL465	O20	2.1
				VAL512	H21	2.1
					O21	1.8
				SER508	O23	2.3
	CUR	−8.32	7	ASN414	O20	2.3
				ASN382	O20	2.1
					O21	2.5
				GLY367	O22	1.8
				VAL606	O22	2.1
					H23	2.4
				ILE559	O23	2.1

incubated with primary antibodies against CYP2E1 (1:1000), Keap1 (1:1000), Nrf2 (1:1000), HO-1 (1:1000), NQO1 (1:1000), GCLC (1:1000), GCLM (1:500) and GAPDH (1:1000) at 4 °C overnight. Then membranes were washed with TBST for three times and incubated with HRP-conjugated anti-rabbit antibodies (1:3000) at room temperature for 1 h. Immunolabelled proteins were revealed by ECL reagents and photographed with the ChemiDoc™ MP System bio-imaging analyzer (Bio-Rad, American). The relative optical densities were analyzed using Image J software (Rawak Software, Germany). All blots were normalized to GAPDH or Histone H3 expression.

2.9. Total RNA extraction and real-time PCR analysis

Total RNA was extracted from liver tissues using Trizol reagent in accordance with the manufacturer's instructions. NanoDrop 2000 ultramicrospectrophotometer (Thermo, American) was used to measure the concentration and purity of the extracted RNA. Subsequently, cDNA was reversely transcripted from 1 μg of total RNA using FastKing RT kit in accordance with the manufacturer's instructions. The cDNA was reversed at −20 °C for subsequent analysis.

Real-time PCR was performed with ChamQ Universal SYBR qPCR Master Mix according to the manufacturer's instructions in the CFX 96 Real-Time PCR Detection System (Bio-Rad, American). The primer sequences were shown in Table 1. The expression of target genes for each group was normalized to the GAPDH gene.

2.10. Molecular docking simulation

Molecular docking assay was carried out to investigate the potential interaction between candidate compounds (OHC, THC and CUR) and the target proteins (CYP2E1 and Keap1) by the AutoDock 4.26 software. The crystal structures of CYP2E1 (PDB ID: 3E6I) and Keap1-inhibitor complex (PDB ID: 5FNU) were derived from the RCSB Protein Data Bank (https://www.rcsb.org/). The 3D structures of OHC (PubChem CID: 13888132), THC (PubChem: CID 124072) and CUR (PubChem CID: 969516) were obtained from the PubChem database (https://pubchem.ncbi.nlm.nih.gov/). The grid boxes were 30 × 30 × 30 Å, computed with a grid spacing of 0.375 Å. The search was carried out with the Lamarckian Genetic Algorithm, populations of 150 individuals and maximum number of energy 2.5×10^6. Besides, a mutation rate of 0.02 has been evolved for 10 generations in each docking. A root mean square deviation (RMSD) tolerance for each cycle was set at 2.0 Å. The interaction between ligands and proteins was evaluated by sorting the different complexes with respect to the predicted binding energy (kcal/mol).

2.11. Statistical analysis

All data were presented as the mean ± standard deviation (SD). Statistical comparisons between mean values of individual groups were carried out using one-way analysis of variance (ANOVA) with Duncan's multiple range tests by IBM SPSS. $p < 0.05$ means the difference has reached statistical significance.

3. Results

3.1. Protective effects of OHC and THC against APAP-induced hepatotoxicity

Serum AST and ALT levels are vital indicators for the evaluation of liver function. As shown in Fig. 2, as anticipated, APAP overdose obviously induced liver injury with increased AST and ALT levels (all $p < 0.01$). However, pretreatment with OHC and THC significantly decreased the elevated AST and ALT levels in a dose-dependent manner in mice, indicative of relieved hepatotoxicity (all $p < 0.01$). Moreover, OHC even regulated liver function to resemble physiological condition (100 mg/kg, $p > 0.05$). It was worthwhile to note that THC and OHC exhibited similar effect as CUR in reducing AST level at a low dose of 50 mg/kg (all $p > 0.05$). THC showed more profound effect than CUR at a dose of 100 mg/kg in decreasing ALT level ($p < 0.05$). OHC also exhibited superior effect to CUR at doses of 50 and 100 mg/kg in attenuating ALT level ($p < 0.05$ for 50 mg/kg; $p < 0.01$ for 100 mg/kg).

The liver histological alterations were exhibited in Fig. 3. When compared with the control group, administration with APAP induced obvious disarrangement of hepatic cells, extensive hepatocyte vacuolation, inflammatory cell infiltration and sinusoidal dilation. However, OHC and THC pretreatment remarkably impeded the deleterious alternations, massively reduced the disarrangement of hepatic cells, decreased hepatocyte vacuolation and diminished sinusoidal dilation. The incidence and severity of histopathological deteriorations in the OHC and THC pretreatment groups were obviously lower than those of CUR group at the same dose (100 mg/kg). Importantly, pretreatment with OHC (100 mg/kg) substantially attenuated liver histopathological alterations. The obvious differential protective effects on liver function and histological deterioration indicated that OHC and THC possessed more appreciable protective effect against APAP-induced hepatotoxicity in parallel to CUR.

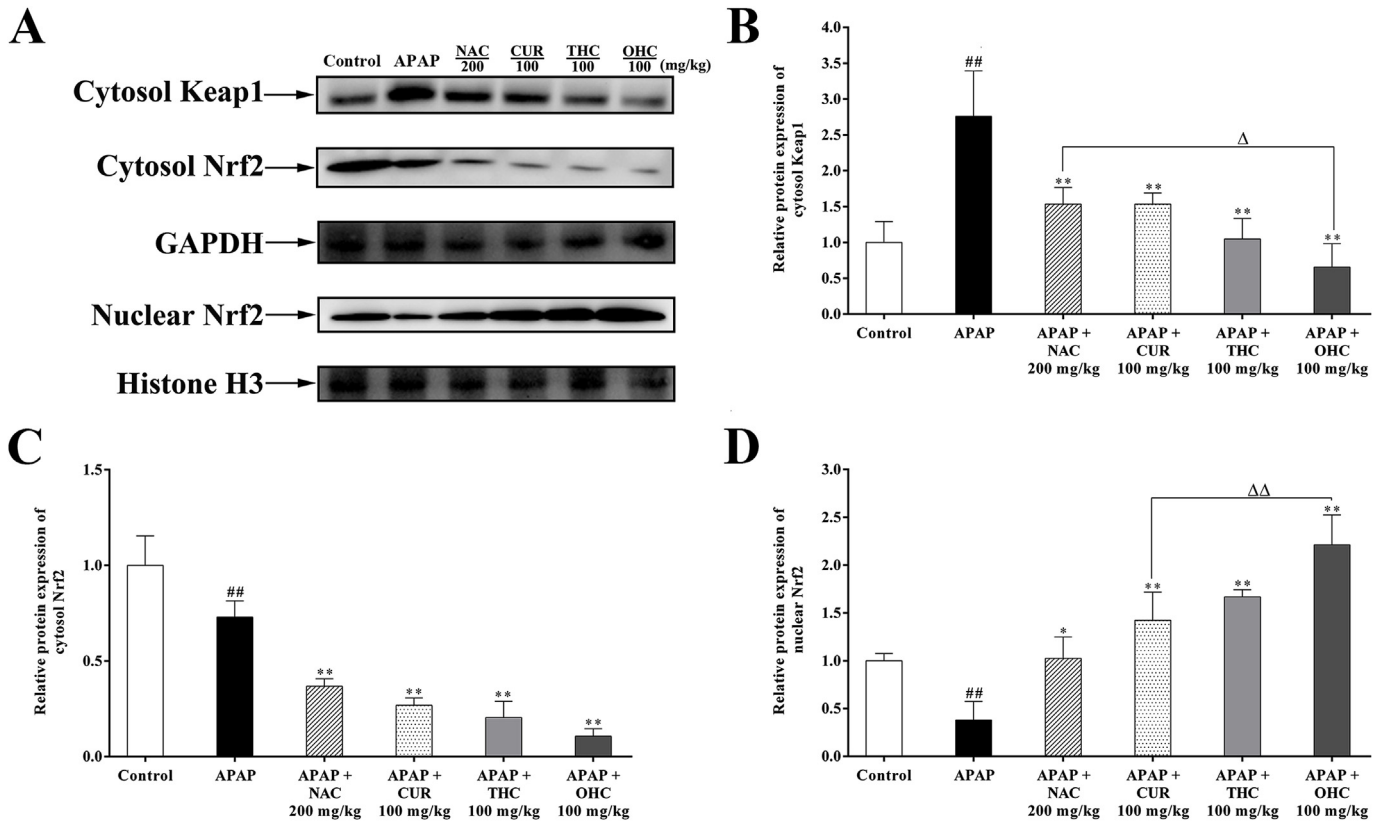

Fig. 6. Differential effects of THC, OHC and CUR on the Keap1-Nrf2 pathway in liver. (A) Representative protein expression bands of Keap1 and Nrf2; (B) Cytosolic Keap1 protein level; (C) Cytosolic Nrf2 protein level; (D) Nuclear Nrf2 protein level. Data are presented as the mean ± SD (n = 3). $^{\#\#}p < 0.01$ versus control group. $^{*}p < 0.05$, $^{**}p < 0.01$ versus APAP-treated group. $^{\Delta}p < 0.05$, $^{\Delta\Delta}p < 0.01$ versus treatment of CUR group.

3.2. Effects of OHC and THC on liver antioxidant status

Changes in MDA contents could reflect the oxidative damage to cell membrane lipids. Fig. 4A showed that APAP significantly enhanced the liver MDA level ($p < 0.01$). However, administration with OHC and THC markedly decreased the hepatic MDA content in a dose-dependent manner (all $p < 0.01$). OHC and THC reduced MDA content to the level similar to that of CUR at a low dose of 25 mg/kg (all $p > 0.05$). Importantly, THC showed more profound inhibitory effect than CUR at the same dose of 100 mg/kg ($p < 0.05$). While OHC exhibited superior anti-lipid peroxidation effect to CUR at doses of 50 and 100 mg/kg ($p < 0.05$ for 50 mg/kg; $p < 0.01$ for 100 mg/kg).

GSH, SOD, CAT are known as the primary antioxidant enzymes. Besides, GSH is the antidote of NAPQI, and T-AOC can reflect the total antioxidant capacity. As shown in Fig. 4B–E, administration with APAP significantly decreased the levels of GSH, SOD, CAT and T-AOC (all $p < 0.01$) as compared with the control group. In contrast, pretreatment with OHC and THC obviously restored levels of these antioxidant indexes at doses of 50 and 100 mg/kg (all $p < 0.01$). The restorative capacity of OHC on GSH, SOD and CAT was more pronounced than that of CUR at 100 mg/kg ($p < 0.05$ for GSH; $p < 0.01$ for SOD; $p < 0.05$ for CAT).

NAPQI adducts with mitochondrial proteins leading to ROS formation. As shown in Fig. 4F, APAP treatment significantly increased the level of ROS as compared to the control group ($p < 0.01$). Nevertheless, pretreatment with OHC and THC at a dose of 100 mg/kg apparently decreased the ROS level in parallel to the APAP group (all $p < 0.01$). Importantly, THC and OHC exhibited more appreciable effect in decreasing ROS level relative to CUR at the same dose (all $p < 0.01$), which indicated that THC and OHC might possess superior antioxidant effect to CUR against APAP-induced liver injury.

3.3. Effects of OHC and THC on CYP2E1 expression and molecular docking analysis

Excessive intake of APAP can be metabolized into NAPQI mainly through CYP2E1. As shown in Fig. 5A, APAP overdose significantly decreased the CYP2E1 activity ($p < 0.01$), which might result from the hepatocellular damage caused by APAP (Xie et al., 2016). Although pretreatment with CUR and THC exhibited differential CYP2E1 inhibitory activities, the difference failed to reach statistical significance. However, pretreatment with OHC obviously inhibited the CYP2E1 activity ($p < 0.01$), about 2-fold lower than that of the APAP group. Fig. 5B–D also revealed that 220 mg/kg APAP significantly up-regulated the gene and protein expressions of CYP2E1 by over 2-fold as compared with the control (all $p < 0.05$). However, OHC and THC pretreatment provoked a 2–3 fold down-regulation on the transcriptional and translational expressions of CYP2E1 relative to the APAP group ($p < 0.01$ for mRNA; $p < 0.05$ for protein).

Furthermore, THC normalized the CYP2E1 gene and protein overexpressions to closely resemble normal levels ($p > 0.05$). OHC even exhibited approximately 2-fold suppressive effect on the gene and protein expressions of CYP2E1 when compared with the control group ($p < 0.01$ for gene; $p < 0.05$ for protein). Noteworthily, OHC and THC both exhibited stronger effect than CUR in inhibiting CYP2E1 mRNA expression (all $p < 0.01$), which was in concert with the comparative effects of THC, OHC and CUR on liver ALT levels, histological alternation, and antioxidant status.

Molecular docking study further indicated that OHC, THC and CUR all interacted with the active site of CYP2E1 with binding energy of −6.11, −5.7 and −6.21 kcal/mol, respectively (Table 2 and Fig. 5E-L). OHC formed hydrogen bonds with the amino acid SER366 of CYP2E1. THC formed hydrogen bonds with ARG344, GLY411 and ASN143 residues. CUR also made hydrogen contact with LEU215, ASN219 and

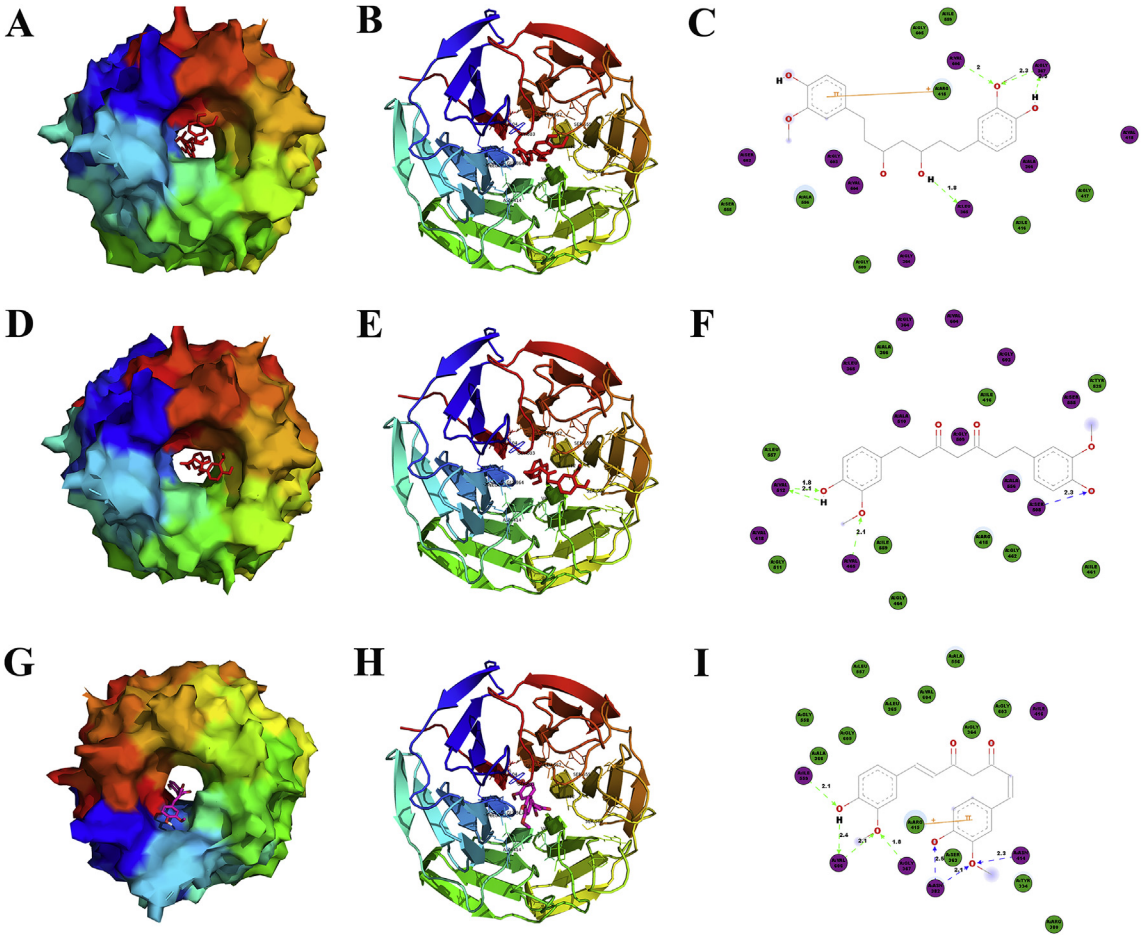

Fig. 7. Molecular docking results of the (A) schematic diagram, (B) 3D and (C) 2D diagrams of the hydrogen bond interaction between OHC and Keap1; (D) schematic diagram, (E) 3D and (F) 2D diagrams of the hydrogen bond interaction between THC and Keap1; (G) schematic diagram, (H) 3D and (I) 2D diagrams of the hydrogen bond interaction between CUR and Keap1.

SER366. These results suggested that OHC and THC revealed distinct affinities to the binding sites as CYP2E1 inhibitors, which was congruent with the *in vivo* enzymatic activity and transcriptional and translational expression levels.

3.4. Effects of OHC and THC on the activation of Keap1-Nrf2 pathway and molecular docking simulation

Keap1 functions as a negative regulator of Nrf2 by binding to Nrf2 in the cytoplasm and promoting its degradation. As shown in Fig. 6B, treatment with APAP resulted in an increase in the expression of cytosolic Keap1 by over 2-fold as compared with the control group ($p < 0.01$). However, pretreatment with OHC, THC and CUR all remarkably suppressed the cytosolic Keap1 protein expression (all $p < 0.01$). Besides, THC and OHC down-regulated the cytosolic Keap1 expression to closely resemble normal level (all $p > 0.05$).

As exhibited in Fig. 6C–D, down-regulated expression of Nrf2 in the nucleus and cytoplasm were observed in the APAP-treated group (all $p < 0.01$). However, OHC, THC and CUR all substantially increased the nuclear Nrf2 and decreased the cytosolic Nrf2 protein expression levels (all $p < 0.01$), indicative of the activation of Keap1-Nrf2 pathway. Noteworthily, OHC exhibited a greater inhibitory effect on cytosolic Keap1 protein expression and a superior effect on promoting the Nrf2 translocation as compared to CUR ($p < 0.05$ for cytosolic Keap1; $p < 0.01$ for nuclear Nrf2).

Moreover, the in silico molecular docking simulation predicted that OHC, THC and CUR all slided into the crystal structure of Keap1 and disturbed the protein-protein interaction between Keap1 and Nrf2, with the binding energy of −5.11, −7.01 and −8.32 kcal/mol, respectively (Table 2 and Fig. 7). Specifically, OHC showed hydrophobic interaction with LEU365, VAL606 and GLY367 of Keap1. THC formed hydrogen bonds with VAL465 and SER508. CUR bound with ASN414, ASN382, VAL606, ILE559, and GLY367. The result indicated that OHC and THC could insert into the pocket of Keap1 and occupy part of the binding site of Nrf2, therefore disturbing the binding of Keap1 to Nrf2 and resulting in the activation of Nrf2, which was in line with the *in vivo* assay.

3.5. Effects of OHC and THC on Nrf2-targeted genes expressions

Nrf2 translocates into the nucleus and induces the expressions of GCLC, GCLM, NQO1 and HO-1 to detoxify and curb the ROS detrimental effect. Glutamate cysteine ligase (GCL), composed of a catalytic (GCLC) and a modifier (GCLM) subunit, is the key determinant of GSH synthesis (Lu, 2009). In the present work, treatment with APAP significantly inhibited the mRNA and protein expressions of GCLC and GCLM (Fig. 8, all $p < 0.01$). In contrast, pretreatment with OHC, THC and CUR all markedly up-regulated the gene expressions of GCLC and GCLM (Fig. 8A, all $p < 0.05$). THC and OHC both obviously enhanced the protein expressions of GCLC and GCLM (Fig. 8C, $p < 0.05$ for GCLC, $p < 0.01$ for GCLM). While CUR only induced significant protein expression of GCLM (Fig. 8C, $p < 0.01$). Impressively, THC showed stronger enhancing effect than CUR on the gene and protein expressions of GCLM (Fig. 8A–C, $p < 0.05$ for gene, $p < 0.01$ for protein). While OHC elicited more obvious effect than CUR in stimulating the gene expressions of GCLC and GCLM, and protein expression of GCLM (Fig. 8A–C, all $p < 0.01$). The differential effects of CUR, THC

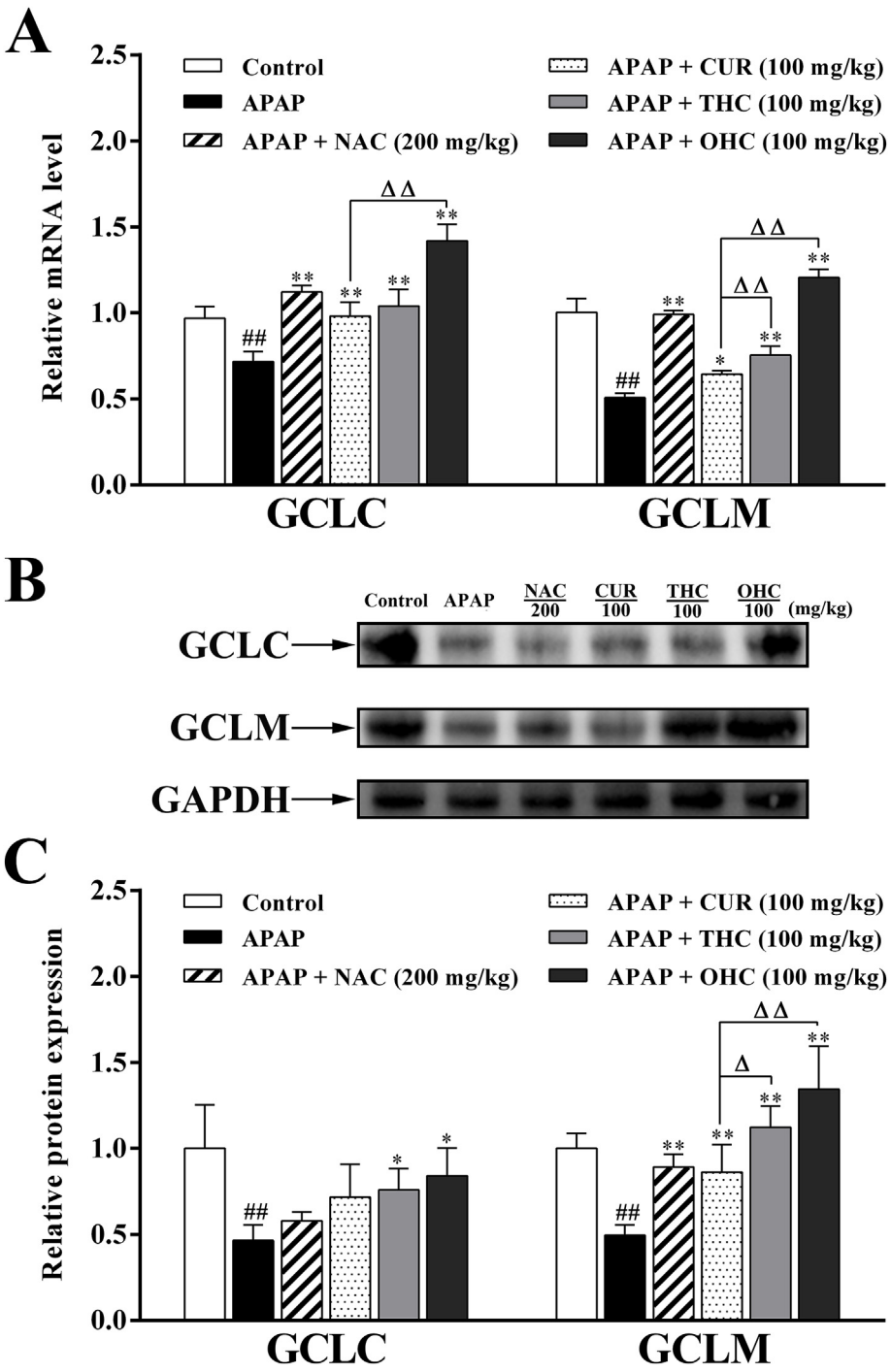

Fig. 8. Differential effects of THC, OHC and CUR on GCL expression in liver. (A) mRNA levels of CGLC and GCLM; (B) Representative protein expression bands of GCLC and GCLM; (C) Protein levels of CGLC and GCLM. Data are presented as the mean ± SD (n = 3). $^{\#\#}p < 0.01$ versus control group. $^{*}p < 0.05$, $^{**}p < 0.01$ versus APAP-treated group. $^{\Delta}p < 0.05$, $^{\Delta\Delta}p < 0.01$ versus treatment of CUR group.

and OHC on GCL were in line with those on the GSH levels.

NQO1 catalyzes the detoxification of quinones and HO-1 catalyzes the rate-limiting step in heme catabolism. As shown in Fig. 10, APAP overdose obviously inhibited the gene and protein expressions of NQO1 and HO-1 (both $p < 0.01$). Whereas pretreatment with THC significantly enhanced the gene and protein expressions of HO-1 (Fig. 9A–C, all $p < 0.01$), and the enhancing effect on HO-1 gene expression was superior to that of CUR (Fig. 9A, $p < 0.01$). Clearly, pretreatment with OHC significantly induced the gene and protein expressions of NQO1 and HO-1 (all $p < 0.01$), with stimulating effect superior to that of CUR (Fig. 9A–C, all $p < 0.01$). The differential effects of CUR, THC and OHC on NQO1 and HO-1 expressions might result from the inconsistent activatory effect on Keap1-Nrf2 pathway.

4. Discussion

APAP overdose is the most common cause of acute liver failure and drug-induced hepatotoxicity worldwide (Budnitz et al., 2011; Manthripragada et al., 2011). Indeed, APAP-induced hepatotoxicity has served as the most popular, mechanistically well-studied and clinically-relevant liver injury model for testing potential hepato-protective candidates (Du et al., 2016). Oxidative stress is deemed as an essential

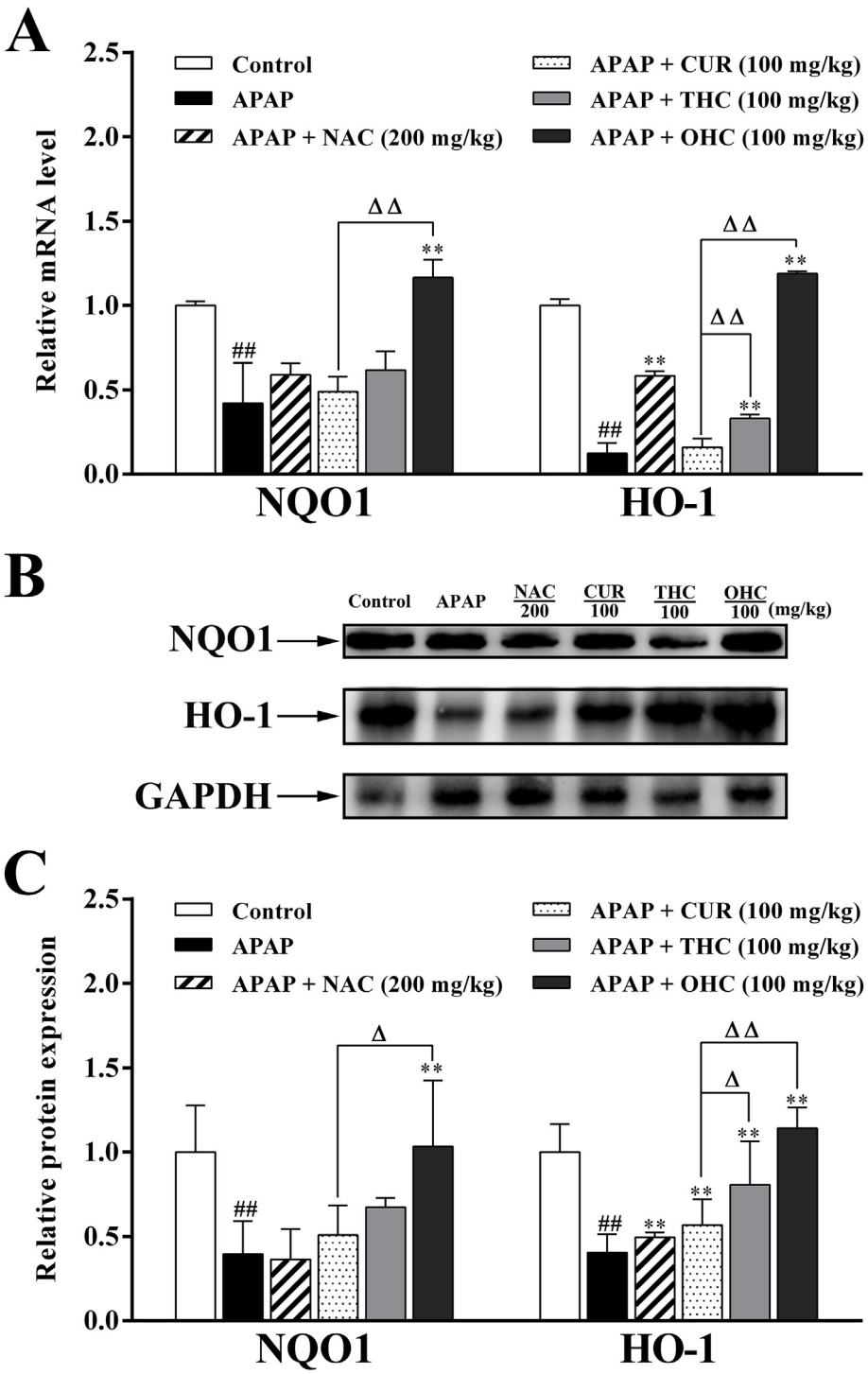

Fig. 9. Differential effects of THC, OHC and CUR on NQO1 and HO-1 expressions in liver. (A) Densitometry analysis of mRNA level; (B) Representative protein expression bands; (C) Densitometry analysis of protein level. Data are presented as the mean ± SD (n = 3). $^{\#\#}p < 0.01$ versus control group. $^{*}p < 0.05$, $^{**}p < 0.01$ versus APAP-treated group. $^{\Delta}p < 0.05$, $^{\Delta\Delta}p < 0.01$ versus treatment of CUR group.

toxicological mechanism for APAP. Hence, many food-derived compounds have been evaluated for their antioxidant activities to protect against APAP-induced hepatotoxicity, such as pyridoxine and sulforaphane (Roh et al., 2018; Wang et al., 2017). CUR, a natural polyphenol compound and food pigment with antioxidant activity, is known for its excellent hepato-protective effect against liver diseases (Li et al., 2018). THC and OHC, the primary and final hydrogenated metabolites of CUR with superior antioxidant activity *in vitro*, were deemed to have potential hepato-protective effect (Somparn et al., 2007). In this study, we followed our previously-established regime to efficiently produce OHC, and comparatively investigated the therapeutic benefits and mechanisms of OHC and THC against APAP-induced hepatotoxicity, by exploring their modulatory effects on serum hepatic indicators, microstructure, redox equilibrium, CYP450 enzyme CYP2E1 and Keap1-Nrf2 pathway, thereby illuminating the potential underlying mechanism of action at the molecular level (Fig. 10).

Our result indicated that OHC and THC pretreatment exerted notable hepato-protective effects against APAP-elicited hepatotoxicity, as

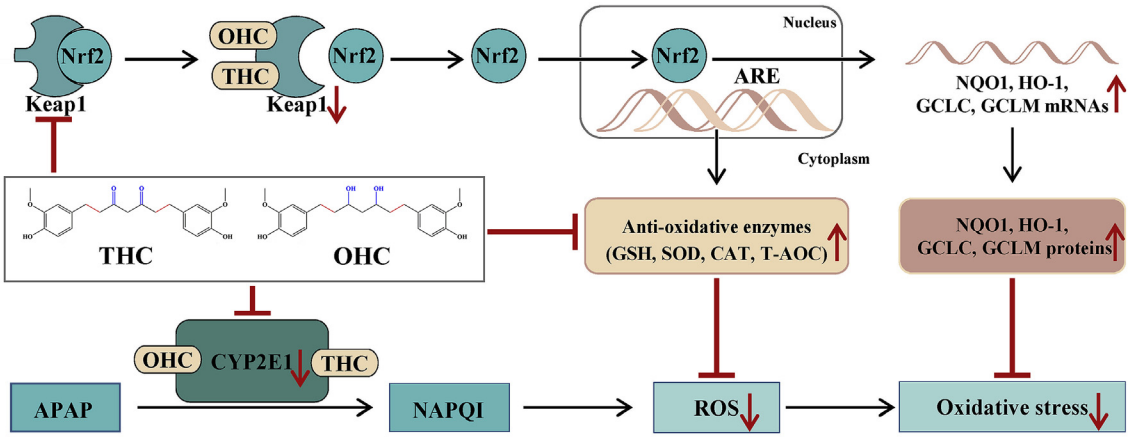

Fig. 10. Schematic representation of proposed mechanism of OHC and THC on the prevention of APAP-induced liver injury. OHC and THC bind to CYP2E1 and inhibit its expression, supposedly attenuating CYP-mediated APAP bio-activation. OHC and THC suppress Keap1 expression, and interact with Keap1, disturbing the protein-protein interaction between Keap1 and Nrf2, thus leading to the translocation of Nrf2 from cytoplasm to the nucleus. Nrf2 activation induces the transcription of its downstream antioxidant response elements (CGLC, GCLM, NQO1 and HO-1), and elevates their translational levels. Activation of Keap1-Nrf2 antioxidant signaling pathway promotes the endogenous antioxidants and quenches the oxidative stress. All the above actions collectively contribute to preserving the redox equilibrium against APAP-induced hepatotoxicity.

evidenced by significantly decreased levels of AST and ALT, and obviously attenuated hepatic histopathological deterioration. OHC and THC seemed to exert superior hepato-protective effect to CUR against APAP overdose. It is well-known that excessive APAP is metabolized into NAPQI mainly through CYP2E1 (Vermeulen et al., 1992). Therefore, suppression of CYP2E1 activity or its expression can alleviate liver injury by decreasing NAPQI formation (Ko et al., 2017). To investigate whether OHC and THC had any effect on CYP2E1, the activity, and gene and protein expressions of CYP2E1 were investigated. Result indicated that OHC and THC both significantly inhibited the mRNA and protein expressions of CYP2E1 (Fig. 5B–D, all $p < 0.05$). Importantly, OHC and THC exhibited a more profound suppressive effect than CUR on CYP2E1 mRNA expression (Fig. 5B, all $p < 0.01$). OHC also possessed superior inhibitory effect on CYP2E1 activity to CUR (Fig. 5A, $p < 0.01$). Molecular docking analysis further revealed that OHC and THC bound to the active sites and interacted with important amino acid residues including SER366, ASN143 and ARG344, which might contribute to the inhibition of CYP2E1 activity. Hence, the suppressive effect of OHC and THC on CYP2E1 might play an important role in the inactivation of APAP biotransformation, therefore contributing to their hepato-protective effect and detoxification against APAP intoxication (Du et al., 2016).

The disequilibrium between the oxidative stress and antioxidant defense system is the leading cue in the progression of varied hepatic disorders. Previous study has proved that APAP overdose generated excessive NAPQI, which subsequently adducted with mitochondrial proteins, leading to ROS formation and oxidant stress (Du et al., 2016). Excessive ROS can be scavenged by the antioxidant systems including low-molecular-weight antioxidants (such as GSH), and enzymes (such as SOD and CAT) (Ma, 2013). In the present study, as expected, APAP overdose resulted in oxidative stress with significantly elevated ROS and MDA levels. In contrast, pretreatment with THC and OHC significantly decreased the hepatic MDA and ROS levels, substantially promoted the liver endogenous antioxidants GSH, SOD and CAT, and improved the scavenging T-AOC, collectively contributing to the alleviation of oxidative stress. It should be noted that THC possessed more pronounced antioxidant activity than CUR *in vivo*, which could be illustrated from obviously lower levels of MDA (Fig. 4A, $p < 0.05$). OHC also possessed stronger intrinsic antioxidant activity than CUR, which could be manifested by significantly lower levels of MDA, and markedly higher levels of GSH, SOD and CAT (Fig. 4A–D, all $p < 0.05$). Hence, THC and OHC could effectively restore the cellular redox balance in APAP-intoxicated mice liver.

Nrf2 serves as the master regulator of endogenous antioxidant defense. Under physiological condition, Nrf2 binds to Keap1 in the cytoplasm, remaining inactivated and easily degraded (Sha et al., 2015). In response to oxidative stress, Nrf2 is released from Keap1 and translocates into nucleus, inducing the transcription of a series of antioxidant genes such as HO-1, NQO1 and GCL (Zhang et al., 2016). Therefore, inhibition of Keap1 or protein-protein interaction between Keap1 and Nrf2 can active the Keap1-Nrf2 pathway against oxidative stress. In the current work, pretreatment with OHC and THC significantly inhibited the Keap1 protein expression, leading to the decreased degradation of Nrf2 (Fig. 6, all $p < 0.01$). Furthermore, molecular docking results suggested that OHC and THC could insert into Keap1 crustal structure and occupy the Nrf2 binding site on Keap1 protein by forming hydrogen bonds with specific residues within Keap1 protein, thus leading to the dissociation of Keap1 with Nrf2 (Fig. 7). All of these led to the translocation of Nrf2 into nucleus, inducing the expressions of a host of Nrf2-targeted genes including GCLC, GCLM, NQO1 and HO-1 (Figs. 8 and 9). It should be noted that THC was more effective than CUR in promoting the gene expression of HO-1 (Fig. 9A, $p < 0.01$), and gene and protein expressions of GCLM (Fig. 8, $p < 0.05$ & $p < 0.01$). Moreover, OHC showed superior effect to CUR in up-regulating the gene expression of GCLC (Fig. 8, $p < 0.01$), and gene and protein expressions of GCLM (Fig. 9, both $p < 0.01$), NQO1 (Fig. 9, $p < 0.01$ & $p < 0.05$), and HO-1 (Fig. 9, both $p < 0.01$). Herewith, OHC and THC were supposed to restore the hepatic antioxidant status through activation of Keap1-Nrf2 signaling pathway, thereby curbing ROS detrimental effect and subsequently hindering the exacerbation of APAP-induced liver damage.

Extensive literature have established that the metabolites of CUR contributed a lot to its bioactivities (Shen and Ji, 2012; Shen et al., 2016). As the primary and final hydrogenated metabolites of CUR, the important role of OHC and THC in CUR's hepato-protective effect were revealed in the present study. Generally, CUR shares analogous structure with THC and OHC, but differs in the presence of β-diketone groups and α, β dienes (Fig. 1). Our comparative evaluation revealed that hydrogenation of the heptadiene moiety of CUR remarkably enhanced the hepato-protective effect (OHC and THC vs. CUR), while the hydrogenation of β-diketone caused only a slight change in the hepato-protective activity (THC vs. OHC).

In spite of the extensive bioactivities, the clinical application of CUR is restricted by its poor bioavailability, which is largely ascribed to its hydrophobic nature (Kocaadam and Sanlier, 2017). It should be noteworthy that THC and OHC have superior aqueous solubility and

stability to their precursor CUR due to the hydrogenated α, β dienes and/or β-diketone (Lin et al., 2010; Saradhi et al., 2010). Herewith, the hydrogenation of heptadiene moiety and the associated aqueous solubility might perform a more preferable role in enhancing the antioxidant and hepato-protective effect of CUR *in vivo*, which was congruent with the antioxidant activities of CUR *in vitro* to some extent (Somparn et al., 2007). Taken together, the superior hepato-protective effect of THC and OHC to CUR might be intimately linked to the hydrogenation of heptadiene, the improved aqueous solubility and the enhanced antioxidant activities.

Overall, we have proved for the first time that food-derived OHC and THC possess pronounced hepato-protective effect against APAP-induced acute liver injury mainly through CYP2E1 suppression and Keap1-Nrf2 pathway activation (Fig. 10). OHC and THC have great potential as novel antioxidants to treat oxidative stress-related liver disorders, especially in the prevention and treatment of APAP-induced hepatotoxicity. Besides, the superior hepato-protective effect revealed in the present study evidently suggests that OHC and THC might be the active antioxidant form of CUR and play an important role in the hepato-protective activities of CUR against APAP-induced hepatotoxicity *in vivo*, which buttresses the rationale for the medicinal application of turmeric as a functional food and dietary therapy for the treatment of liver diseases. The favorable aqueous solubility and superior antioxidant and hepato-protective activities *in vivo* indicates that OHC and THC could serve as promising lead template scaffolds for the design of novel curcumin analogs.

Conflicts of interest

The authors declare that there are no conflicts of interest.

CRediT authorship contribution statement

Dan-Dan Luo: formal analysis, Writing – original draft. **Jin-Fen Chen:** formal analysis, Methodology. **Jing-Jing Liu:** Methodology. **Jian-Hui Xie:** Writing ? review & editing. **Zhen-Biao Zhang:** Methodology. **Jiang-Yong Gu:** Software. **Jian-Yi Zhuo:** Methodology. **Zi-Ren Su:** Supervision, Resources. **Zhang-Hua Sun:** Conceptualization, Resources.

Acknowledgement

This work was supported by grants from National Key R&D Program of China (No. 2017YFC0506200), Science and Technology Development Special Project of Guangdong Province (No. 2017A050506044), Guangdong Provincial Department of Education Feature Innovation Project (No. 2016KTSCX018), and Science and Technology Project of Guangzhou (No. 201704030028).

Transparency document

Transparency document related to this article can be found online at https://doi.org/10.1016/j.fct.2018.11.012.

References

Bray, B.J., Rosengren, R.J., 2001. Retinol potentiates acetaminophen-induced hepatotoxicity in the mouse: mechanistic studies. Toxicol. Appl. Pharmacol. 173, 129–136.
Budnitz, D.S., Lovegrove, M.C., Crosby, A.E., 2011. Emergency department visits for overdoses of acetaminophen-containing products. Am. J. Prev. Med. 40, 585–592.
Das, S., Roy, P., Auddy, R.G., Mukherjee, A., 2011. Silymarin nanoparticle prevents paracetamol-induced hepatotoxicity. Int. J. Nanomed. 6, 1291–1301.
Du, K., Ramachandran, A., Jaeschke, H., 2016. Oxidative stress during acetaminophen hepatotoxicity: sources, pathophysiological role and therapeutic potential. Redox. Biol. 10, 148–156.
Ireson, C.R., Jones, D.J.L., Orr, S., Coughtrie, M.W.H., Boocock, D.J., Williams, M.L., Farmer, P.B., Steward, W.P., Gescher, A.J., 2002. Metabolism of the cancer chemopreventive agent curcumin in human and rat intestine. Cancer. Epidem. Biomar. 11, 105–111.
Kaspar, J.W., Niture, S.K., Jaiswal, A.K., 2009. Nrf2:INrf2 (Keap1) signaling in oxidative stress. Free Radic. Biol. Med. 47, 1304–1309.
Ko, J.W., Shin, J.Y., Kim, J.W., Park, S.H., Shin, N.R., Lee, I.C., Shin, I.S., Moon, C., Kim, S.H., Kim, S.H., 2017. Protective effects of diallyl disulfide against acetaminophen-induced nephrotoxicity: a possible role of CYP2E1 and NF-κB. Food Chem. Toxicol. 102, 156–165.
Kocaadam, B.L., Sanlier, N., 2017. Curcumin, an active component of turmeric (Curcuma longa), and its effects on health. Crit. Rev. Food Sci. Nutr. 57, 2889–2895.
Kong, S.Z., Lin, G.S., Liu, J.J., Su, L.Y., Zeng, L., Luo, D.D., Su, Z.R., Wang, H.F., 2018. Hepatoprotective effect of ultrafine powder of Dendrobium officinale against acetaminophen-induced liver injury in mice. Food Sci. Technol. Res. 24, 339–346.
Lancaster, E.M., Hiatt, J.R., Zarrinpar, A., 2015. Acetaminophen hepatotoxicity: an updated review. Arch. Toxicol. 89, 193–199.
Lee, W.M., 2017. Public health: acetaminophen (APAP) hepatotoxicity- isn't it time for APAP to go away? J. Hepatol. 67, 1324–1331.
Leong, P.K., Chiu, P.Y., Ko, K.M., 2012. Prooxidant-induced glutathione antioxidant response in vitro and in vivo: a comparative study between schisandrin B and curcumin. Biol. Pharm. Bull. 35, 464–472.
Li, S., Tan, H.Y., Wang, N., Cheung, F., Hong, M., Feng, Y.B., 2018. The potential and action mechanism of polyphenols in the treatment of liver diseases. Oxid. Med. Cell. Longev., 8394818 2018.
Lin, J.K., Pan, M.H., Linshiau, S.Y., 2010. Recent studies on the biofunctions and biotransformations of curcumin. Biofactors 13, 153–158.
Lin, G.S., Luo, D.D., Liu, J.J., Wu, X.L., Chen, J.F., Huang, Q.H., Su, L.Y., Zeng, L., Wang, H.F., Su, Z.R., 2018. Hepatoprotective effect of polysaccharides isolated from dendrobium officinale against acetaminophen-induced liver injury in mice via regulation of the Nrf2-Keap1 signaling pathway. Oxid. Med. Cell. Longev., 6962439 2018.
Liu, Y., Chen, L.Y., Shen, Y., Tan, T., Xie, N.Z., Luo, M., Li, Z.H., Xie, X.Y., 2016. Curcumin ameliorates ischemia-induced limb injury through immunomodulation. Med. Sci. Mon. Int. Med. J. Exp. Clin. Res. 22, 2035–2042.
Liu, W.H., Zhang, Z.B., Lin, G.S., Luo, D.D., Chen, H.B., Yang, H.M., Liang, J.L., Liu, Y.H., Xie, J.H., Su, Z.R., 2017. Tetrahydrocurcumin is more effective than curcumin in inducing the apoptosis of H22 cells via regulation of a mitochondrial apoptosis pathway in ascites tumor-bearing mice. Food. Funct. 8, 3120–3129.
Lu, S.C., 2009. Regulation of glutathione synthesis. Mol. Aspect. Med. 30, 42–59.
Lu, M.C., Ji, J.A., Jiang, Z.Y., You, Q.D., 2016. The Keap1-Nrf2-ARE pathway as a potential preventive and therapeutic target: an update. Med. Res. Rev. 36, 924–963.
Ma, Q., 2013. Role of Nrf2 in oxidative stress and toxicity. Annu. Rev. Pharmacol. Toxicol. 53, 401–426.
Manthripragada, A.D., Zhou, E.H., Budnitz, D.S., Lovegrove, M.C., Willy, M.E., 2011. Characterization of acetaminophen overdose-related emergency department visits and hospitalizations in the United States. Pharmacoepidemiol. Drug Saf. 20, 819–826.
Murugan, P., Pari, L., 2010. Influence of tetrahydrocurcumin on hepatic and renal functional markers and protein levels in experimental type 2 diabetic rats. Basic Clin. Pharmacol. Toxicol. 101, 241–245.
Nakmareong, S., Kukongviriyapan, U., Pakdeechote, P., Donpunha, W., Kukongviriyapan, V., Kongyingyoes, B., Sompamit, K., Phisalaphong, C., 2011. Antioxidant and vascular protective effects of curcumin and tetrahydrocurcumin in rats with L-NAME-induced hypertension. Naunyn-Schmiedeberg's Arch. Pharmacol. 383, 519–529.
Oh, S.W., Cha, J.Y., Jung, J.E., Chang, B.C., Kwon, H.J., Lee, B.R., Kim, D.Y., 2011. Curcumin attenuates allergic airway inflammation and hyper-responsiveness in mice through NF-κB inhibition. J. Ethnopharmacol. 136, 414.
Pang, C., Zheng, Z.Y., Shi, L., Sheng, Y.C., Wei, H., Wang, Z.T., Ji, L.L., 2016. Caffeic acid prevents acetaminophen-induced liver injury by activating the Keap1-Nrf2 antioxidative defense system. Free Radical Biol. Med. 91, 236–246.
Pari, L., Murugan, P., 2004. Protective role of tetrahydrocurcumin against erythromycin estolate-induced hepatotoxicity. Pharmacol. Res. 49, 481–486.
Roh, T., De, U., Lim, S.K., Kim, M.K., Choi, S.M., Lim, D.S., Yoon, S., Kacew, S., Kim, H.S., Lee, B.M., 2018. Detoxifying effect of pyridoxine on acetaminophen-induced hepatotoxicity via suppressing oxidative stress injury. Food Chem. Toxicol. 114, 11–22.
Saradhi, U.V.R.V., Ling, Y.H., Wang, J., Chiu, M., Schwartz, E.B., Fuchs, J.R., Chan, K.K., Liu, Z.F., 2010. A liquid chromatography-tandem mass spectrometric method for quantification of curcuminoids in cell medium and mouse plasma. J. Chromatogr. B. Analyt. Technol. Biomed. Life. Sci. 878, 3045–3051.
Sha, L., Tan, H.Y., Ning, W., Zhang, Z.J., Lao, L., Wong, C.W., Feng, Y., 2015. The role of oxidative stress and antioxidants in liver diseases. Int. J. Mol. Sci. 16, 26087–26124.
Shen, L., Ji, H.F., 2012. The pharmacology of curcumin: is it the degradation products? Trends Mol. Med. 18, 138–144.
Shen, L., Liu, C.C., An, C.Y., Ji, H.F., 2016. How does curcumin work with poor bioavailability? Clues from experimental and theoretical studies. Sci. Rep. 6, 20872.
Shin, S.M., Yang, J.H., Ki, S.H., 2013. Role of the Nrf2-ARE pathway in liver diseases. Oxid. Med. Cell. Longev. 763257 2013.
Somparn, P., Phisalaphong, C., Nakornchai, S., Unchern, S., Morales, N.P., 2007. Comparative antioxidant activities of curcumin and its demethoxy and hydrogenated derivatives. Biol. Pharm. Bull. 30, 74–78.
Song, K.I., Park, J.Y., Lee, S., Lee, D., Jang, H.J., Kim, S.N., Ko, H., Kim, H.Y., Lee, J.W., Hwang, G.S., 2015. Protective effect of tetrahydrocurcumin against cisplatin-induced renal damage: in vitro and in vivo studies. Planta Med. 81, 286–291.
Vermeulen, N.P.E., Bessems, J.G.M., Straat, R.V.D., 1992. Molecular aspects of paracetamol-induced hepatotoxicity and its mechanism-based prevention. Drug Metab. Rev. 24, 367–407.
Wang, X., Wu, Q., Liu, A., Anadón, A., Rodríguez, J.L., Martínezlarrañaga, M.R., Yuan, Z., Martínez, M.A., 2017. Paracetamol: overdose-induced oxidative stress toxicity, metabolism, and protective effects of various compounds in vivo and in vitro. Drug

Metab. Rev. 49, 1–83.
Xie, W., Jiang, Z., Jian, W., Zhang, X., Melzig, M.F., 2016. Protective effect of hyperoside against acetaminophen (APAP) induced liver injury through enhancement of APAP clearance. Chem. Biol. Interact. 246, 11–19.
Xu, W., Wu, Q., Liu, A., Anadón, A., Rodríguez, J., Martínezlarrañaga, M., Yuan, Z., Martínez, M., 2017. Paracetamol: overdose-induced oxidative stress toxicity, metabolism, and protective effects of various compounds in vivo and in vitro. Drug. Metab. Rev. 49, 395–437.
Yue, J., Dong, G., He, C., Chen, J., Liu, Y., Peng, R., 2009. Protective effects of thiopronin against isoniazid-induced hepatotoxicity in rats. Toxicology 264, 185–191.
Zhang, R., Xu, M., Wang, Y., Xie, F., Zhang, G., Qin, X., 2016. Nrf2-a promising therapeutic target for defensing against oxidative stress in stroke. Mol. Neurobiol. 54, 6006–6017.
Zhang, Z.B., Luo, D.D., Xie, J.H., Lin, G.S., Zhou, J.T., Liu, W.H., Li, H.L., Yi, T.G., Su, Z.R., Chen, J.P., 2018. Octahydrocurcumin, a final hydrogenated metabolite of curcumin, possesses superior anti-tumor activity through induction of cellular apoptosis. Food. Funct. 25, 2005–2014.
Zhao, F., Gong, Y.D., Hu, Y., Lu, M.H., Wang, J., Dong, J.X., Chen, D.Q., Chen, L., Fu, F.H., Qiu, F., 2015. Curcumin and its major metabolites inhibit the inflammatory response induced by lipopolysaccharide: translocation of nuclear factor-κB as potential target. Mol. Med. Rep. 11, 3087–3093.